



Clinical and Preclinical Single-Dose Pharmacokinetics of VIR-2218, an RNAi Therapeutic Targeting HBV Infection

Sneha V. Gupta¹ · Marie C. Fanget² · Christopher MacLauchlin⁵ · Valerie A. Clausen⁶ · Jing Li⁶ · Daniel Cloutier³ · Ling Shen⁴ · Gabriel J. Robbie⁷ · Erik Mogalian¹

Accepted: 6 October 2021 / Published online: 6 November 2021
© The Author(s) 2021

Abstract

Background and Objective VIR-2218 is an investigational *N*-acetylgalactosamine–conjugated RNA interference therapeutic in development for chronic hepatitis B virus (HBV) infection. VIR-2218 was designed to silence HBV transcripts across all genotypes and uses Enhanced Stabilization Chemistry Plus (ESC+) technology.

This study was designed to evaluate the single-dose pharmacokinetics of VIR-2218 in preclinical species and healthy volunteers.

Methods Preclinically, a single subcutaneous dose of VIR-2218 (10 mg/kg) was administered to rats and nonhuman primates (NHPs), and the pharmacokinetics were assessed in plasma, urine, and liver using standard noncompartmental analysis (NCA) methods. Clinically, healthy volunteers were randomized (6:2 active:placebo) to receive a single subcutaneous dose of VIR-2218 (50–900 mg) or placebo. Pharmacokinetics were similarly assessed within human plasma and urine using NCA methods.

Results In rats and NHPs, VIR-2218 was stable in plasma and was converted to AS(N-1)3'VIR-2218, the most prominent circulating metabolite, at < 10% plasma exposure compared with parent. VIR-2218 rapidly distributed to the liver, reaching peak liver concentrations within 7 and 24 h in rats and NHPs, respectively. In humans, VIR-2218 was rapidly absorbed, with a median time to peak plasma concentration (t_{\max}) of 4–7 h, and had a short median plasma half-life of 2–5 h. Plasma exposures for area under the plasma concentration–time curve up to 12 h (AUC_{0-12}) and mean maximum concentrations (C_{\max}) increased in a slightly greater-than-dose-proportional manner across the dose range studied. Interindividual pharmacokinetic variability was low to moderate, with a percent coefficient of variation of < 32% for AUC and < 43% for C_{\max} . A portion of VIR-2218 was converted to an active metabolite, AS(N-1)3'VIR-2218, with a median t_{\max} of 6–10 h, both of which declined below the lower limit of quantification in plasma within 48 h. The pharmacokinetic profile of AS(N-1)3'VIR-2218 was similar to that of VIR-2218, with plasma AUC_{0-12} and C_{\max} values \leq 12% of VIR-2218. VIR-2218 and AS(N-1)3'VIR-2218 were detectable in urine through the last measured time point, with approximately 17–48% of the administered dose recovered in urine as unchanged VIR-2218 over 0–24 h postdose. Based on pharmacokinetics in preclinical species, VIR-2218 localizes to the liver and likely exhibits prolonged hepatic exposure. Overall, no severe or serious adverse events or discontinuations due to adverse events were observed within the dose range evaluated for VIR-2218 in healthy volunteers (Vir Biotechnology, Inc., unpublished data).

Conclusions VIR-2218 showed favorable pharmacokinetics in healthy volunteers supportive of subcutaneous dosing and continued development in patients with chronic HBV infection.

Clinical Trial Registration No NCT03672188, September 14, 2018.

✉ Sneha V. Gupta
sgupta@vir.bio

Extended author information available on the last page of the article

Key Points

VIR-2218 is an investigational Enhanced Stabilization Chemistry Plus (ESC+) liver-directed RNA interference (RNAi) therapeutic for the treatment of chronic hepatitis B virus (HBV) infection that targets all HBV transcripts.

This study describes the favorable plasma and urine pharmacokinetics of VIR-2218 in healthy volunteers, supportive of subcutaneous dosing and ongoing development.

Prolonged urine collection and analysis provided the first direct pharmacokinetics-based evidence of prolonged exposure for an RNAi therapeutic in healthy volunteers.

1 Introduction

Chronic hepatitis B virus (HBV) infection remains an important global health issue that leads to serious sequelae over time, including cirrhosis, liver failure, and hepatocellular carcinoma [1]. An estimated 257 million people are living with chronic HBV infection worldwide, and approximately 887,000 die from disease-associated complications annually [2, 3]. Despite an available HBV vaccine, perinatal transmission among HBV-infected mothers contributes to the persistence of this virus in the high endemic regions of sub-Saharan Africa and western Pacific regions [4]. Human HBV is a DNA virus in the Hepadnaviridae family with ten HBV genotypes (A to J) that infects, replicates, and persists in human hepatocytes [5, 6]. Current treatment options for chronic HBV infection are limited. The current standard of care for most patients is long-term monotherapy with an HBV polymerase nucleos(t)ide inhibitor (NUC) [7]. Although NUCs suppress viral replication, they do not lead to a functional cure (i.e., loss of hepatitis B surface antigen [HBsAg] in the blood) [8]. An alternative treatment option is a 1-year course of pegylated interferon- α that results in a functional cure in < 10% of patients and is poorly tolerated in the context of the approved 48-week dosing regimen [9]. Given the limitations of current therapies for chronic HBV infection, new treatment modalities that are curative and well-tolerated are needed.

Small interfering ribonucleic acids (siRNA) are a new class of medicines that use the endogenous RNA interference (RNAi) machinery to degrade target messenger RNA (mRNA) transcripts. Generally, synthetic siRNAs are double-stranded oligonucleotides of 19–25 base pairs arranged in a staggered duplex with a 2–4 nucleotide overhang at one

or both of the 3' ends that can be designed to target specific endogenous mRNA molecules. Once inside the cell, the guide (or antisense) strand of the siRNA is incorporated into the RNA-induced silencing complex and binds to its complementary mRNA sequence, directing the enzyme complex to cleave the target mRNA, resulting in reduced protein expression [10, 11].

Unmodified siRNAs are very labile, resulting in rapid degradation, and hence do not achieve appreciable tissue distribution upon systemic administration [12]. However, recent advances in the delivery and metabolic stability of siRNA molecules have improved their pharmacokinetics and bioavailability. For example, chemical alterations to the siRNA that improved its molecular stability and minimized metabolic lability use Enhanced Stabilization Chemistry (ESC), including a combination of phosphorothioate, 2'-*O*-methyl nucleotide, and 2'-fluoro modifications [13, 14]. RNAi compounds synthesized with these types of modifications have shown efficient and sustained reductions of target protein, yielding successful clinical proof of concept in various therapeutic areas [15, 16].

VIR-2218 is an investigational, N-acetylgalactosamine (GalNAc)-conjugated, double-stranded RNAi therapeutic chemically modified using ESC+ that stabilizes the siRNA in vivo and decreases off-target effects. The GalNAc moiety enables targeted delivery of VIR-2218 into the liver via uptake by asialoglycoprotein receptors (ASGPR) expressed primarily and abundantly on the surface of hepatocytes [17]. ASGPR is a high-capacity, highly conserved glycoprotein transporter whose activity remains robust even in settings in which ASGPR levels may be reduced (e.g., cirrhosis, hepatocellular carcinoma) [18]. Binding of the GalNAc ligand to ASGPR leads to receptor-mediated endocytosis of the ligand–receptor complex, followed by release of the siRNA in the endosome and subsequent recycling of the receptor to the cell surface for successive rounds of uptake. VIR-2218 targets the region of the HBV genome that is common to all viral transcripts; thus, VIR-2218 is designed to silence all HBV viral RNAs and is pharmacologically active against HBV genotypes A to J. VIR-2218 has the potential to mediate multiple antiviral effects via the degradation of all HBV transcripts and consequently the reduction of the expression of all HBV proteins, differentiating it from current NUC therapy, which inhibits a single viral target to suppress viral replication but has no significant impact on viral protein expression.

In preclinical studies, absorption, distribution, metabolism, and excretion of VIR-2218 were evaluated after single-dose subcutaneous administration in rats and nonhuman primates (NHPs). Based on the robust HBsAg reduction (Vir Biotechnology, Inc., unpublished data) and favorable pharmacokinetic properties observed in the preclinical studies, VIR-2218 is being assessed in an ongoing, first-in-human,

proof-of-concept phase I/II clinical study evaluating the safety, tolerability, pharmacokinetics, and antiviral activity of VIR-2218 in healthy volunteers and subjects with chronic HBV infection (study VIR-2218-1001; ClinicalTrials.gov identifier: NCT03672188). Here, we report the plasma and urine pharmacokinetics of VIR-2218 and the primary circulating metabolite after a single subcutaneous dose of VIR-2218 in healthy volunteers from the first-in-human, phase I portion of the study.

2 Methods

2.1 Study Design

This portion of the study was a phase I, randomized, double-blind, placebo-controlled, single-ascending-dose study in healthy volunteers enrolled at a study site in New Zealand. The study was sponsored by Vir Biotechnology, Inc. and Alnylam Pharmaceuticals, Inc. and approved by central and local institutional review boards or ethics committees according to the International Conference on Harmonization for Good Clinical Practice, the World Medical Association Declaration of Helsinki, and the 1996 Health Insurance Portability and Accountability Act. All subjects provided written informed consent. The primary objective of the study was to evaluate the safety and tolerability of single doses of VIR-2218, and the secondary objective was to characterize its plasma and urine pharmacokinetics. Selection of doses was based on safety margins calculated from in vivo nonclinical studies in rats and NHPs (Vir Biotechnology, Inc., unpublished data). Within each cohort, subjects were randomized 6:2 (*N* = 8 per cohort) to receive a single ascending dose of subcutaneous VIR-2218 or placebo (50, 100, 200, 400, 600, and 900 mg; Fig. 1). Dose escalation proceeded after

evaluation of the safety and tolerability data obtained from the preceding cohort.

2.2 Study Population

Healthy men and women (aged 18–55 years) with a body mass index (BMI) of 18.0 to ≤ 32 kg/m², normal creatinine clearance (≥ 90 mL/min; Cockcroft–Gault), and no clinically significant medical conditions were enrolled. Subjects were excluded if their liver function test results were outside the normal range.

2.3 Pharmacokinetic Assessments

2.3.1 Preclinical Studies

Plasma pharmacokinetic samples were evaluated in rats and NHPs for VIR-2218 as well as metabolite, AS(N-1)3' VIR-2218, for subsequent pharmacokinetic analysis after a single subcutaneous dose of 10 mg/kg. In rats, blood samples were collected at 1, 3, 7, 24, 72, 168, 336, 504, 672, 840, and 1008 h postdose for subcutaneous administration. In NHPs, blood samples were collected at 0.25, 0.5, 1, 2, 4, 8, 24, 48, 96, 168, 336, and 504 h postdose for subcutaneous administration. Liver tissue samples and urine were also collected for quantitation of VIR-2218 and AS(N-1)3' VIR-2218 for subsequent pharmacokinetic analysis.

2.3.2 Healthy Volunteers

Intensive plasma and urine pharmacokinetic samples were collected for 1 week after administration. Serial samples of plasma were collected 15 min before dosing and at 30 min; at 1, 2, 4, 6, 8, 10, 12, 24, and 48 h; and at 1 week postdose (Fig. 1). Pooled urine samples were collected over 24 h at 0–4, 4–8, 8–12, and 12–24 h, and single void samples were

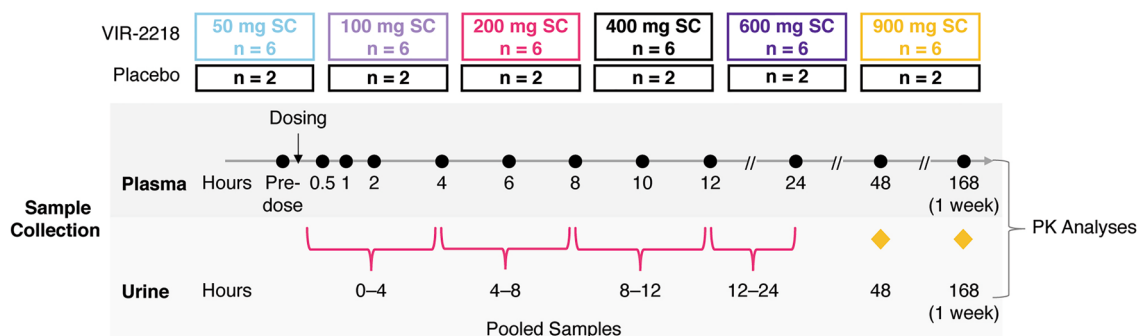


Fig. 1 Study design for VIR-2218 administration in healthy volunteers. Phase I randomized, double-blind, placebo-controlled, single-ascending-dose study in healthy adults who received a single

ascending dose of subcutaneous VIR-2218 or placebo. PK, pharmacokinetic; SC, subcutaneous

also collected at 48 h and 1-week postdose (Fig. 1). All samples were stored at -70°C or below until analysis.

2.3.3 Drug Concentration Assays

Concentrations of VIR-2218 and AS(N-1)3'VIR-2218 in rat and NHP plasma and in human plasma and urine were measured using validated high-performance liquid chromatography time-of-flight mass spectroscopy (LC-TOF-MS) assays with lower limit of quantitation (LLOQ) of 10 ng/mL in plasma and urine. The LC-TOF-MS methods specifically quantified VIR-2218, the full length of the duplex (antisense and sense strands), and A-312327, the single antisense strand of the duplex metabolite AS(N-1)3'VIR-2218, simultaneously. For both plasma and urine, the linear range was 10–10,000 ng/ml (for both VIR-2218 and AS(N-1)3'VIR-2218). For plasma, the analytical quality control (QC) intra-run precision range (% coefficient of variation [CV]) was 3.1–13.8 for VIR-2218 antisense A-163728, 2.5–19.3 for VIR-2218 sense A-133656, and 2.6–13.8 for AS(N-1)3'VIR-2218. The analytical QC inter-run precision range (%CV) was 5.6–13.3 for antisense A-163728, 5.8–15.7 for sense A-133656, and 7.7–14.0 for AS(N-1)3'VIR-2218. Plasma extraction recovery was 60.4% for VIR-2218 antisense A-163728, 58.5% for VIR-2218 sense A-133656, and 91.4% for AS(N-1)3'VIR-2218. For urine, the analytical QC intra-run precision range (%CV) was 1.5–8.2 for VIR-2218 antisense A-163728, 1.0–9.5 for VIR-2218 sense A-133656, and 1.9–12.6 for AS(N-1)3'VIR-2218. The analytical QC inter-run precision range (%CV) was 2.2–6.7 for VIR-2218 antisense A-163728, 4.0–7.9 for VIR-2218 sense A-133656, and 2.8–9.7 for AS(N-1)3'VIR-2218. Urine extraction recovery was 98.3% for VIR-2218 antisense A-163728, 94.2% for VIR-2218 sense A-133656, and 90.5% for AS(N-1)3'VIR-2218.

Concentrations of VIR-2218 and AS(N-1)3'VIR-2218 in rat and monkey urine and liver were measured with similar qualified LC-TOF-MS assays. The LLOQ for the urine assays was 20 ng/mL, and the LLOQ for the liver assays was 200 ng/g.

2.4 Pharmacokinetic and Statistical Analyses

In preclinical studies, noncompartmental pharmacokinetic parameter estimates were determined from mean concentration–time data using Phoenix[®] WinNonlin[®], version 7.0 (Certara USA, Inc; Princeton, NJ, USA). In clinical studies, pharmacokinetic parameters were estimated using standard noncompartmental methods in WinNonlin[®], V8.2.0 (Certara USA, Inc; Princeton, NJ, USA). Pharmacokinetic parameters were assessed in subjects who received VIR-2218 and

had at least one postdose blood sample contributing to evaluable pharmacokinetic data.

The maximum plasma concentration (C_{max}) and time to reach C_{max} (t_{max}) were assessed and observed from the plasma concentration–time data. Calculated pharmacokinetic parameters included area under the plasma concentration–time curve from time zero to time of the last measurable concentration (AUC_t). To estimate the apparent first-order terminal elimination rate constant, λ_z linear regression of concentration in natural logarithmic scale versus time was performed using at least three data points. The linear trapezoidal method was used in the computation of all AUC values, including AUC_t , typically up to 12 or 24 h for all subjects. The following pharmacokinetic parameters were presented only for subjects who exhibited a λ_z in their concentration versus time profiles: half-life ($t_{1/2}$), AUC extrapolated to infinity (AUC_{∞}), apparent plasma clearance (CL/F), and apparent volume of distribution (V_z/F). Subjects with AUC% extrapolation (AUC% extrapol) $> 20\%$ were excluded from the calculation of all elimination-related parameters (λ_z , AUC_{∞} , $t_{1/2}$, CL/F , and V_z/F) from the summary statistics. For urine pharmacokinetics, the cumulative amount of drug excreted in urine (A_e) and the fraction eliminated (f_e), calculated as A_e/dose , were reported. Because pooled urine pharmacokinetic samples were collected up to 24 h in all subjects, renal clearance (CL_R), determined by the ratio of $A_e/\text{plasma AUC}_{0-24}$, was reported.

The C_{max} and AUC of VIR-2218 and AS(N-1)3'VIR-2218 for each cohort were evaluated using a power model for dose proportionality. The power model is described as $\log(y) = \log(\beta_0) + \beta_1 \times \log(\text{dose})_1$, where y , β_0 , and β_1 correspond to the pharmacokinetic variable, proportionality constant, and exponent, respectively. The exponent β_1 in the power model was estimated by regressing the natural log-transformed pharmacokinetic variable on the natural log-transformed dose. Dose proportionality is implied if the 90% confidence interval (CI) for β_1 falls between 0.7 and 1.43 [19].

3 Results

3.1 Pharmacokinetics of VIR-2218 in Preclinical Studies

In preclinical studies, pharmacokinetic parameters of VIR-2218 were evaluated after administration of a single subcutaneous dose of 10 mg/kg in rats and NHPs (Table 1 in electronic supplementary material [ESM]-1). Metabolite profiling studies identified a 3' (N-1) antisense strand metabolite of VIR-2218, AS(N-1)3'VIR-2218, as the primary metabolite of VIR-2218 across plasma, urine, and liver samples in preclinical studies. AS(N-1)3'VIR-2218, formed by the loss of one nucleotide from the 3' end of the antisense

strand of VIR-2218, is expected to have similar potency to VIR-2218 based on evidence from other GalNAc siRNAs with AS(N-1)3' metabolite [20].

After a single subcutaneous dose in male rats, VIR-2218 was rapidly absorbed and eliminated from plasma with a mean t_{\max} of 1.0 h and a $t_{1/2}$ of 6.7 h (Table 2 in ESM-1) with metabolite AS(N-1)3' VIR-2218 below LLOQ. Similarly, plasma absorption and elimination were also rapid after subcutaneous administration in NHPs (t_{\max} 2.6 h; $t_{1/2}$ 2.9 h; Table 2 in ESM-1) with AS(N-1)3' VIR-2218 detected at low levels. VIR-2218 primarily distributed to the liver with much higher exposures than in plasma in both rats and NHPs (Table 1; Table 2 in ESM-1). The $t_{1/2}$ in the liver was significantly longer (93.1 and 160.0 h in rats and NHPs, respectively; Table 1) than that in plasma (6.7 and 2.9 h in rats and NHPs, respectively; Table 2 in ESM-1). Similar to VIR-2218, higher concentrations of AS(N-1)3' VIR-2218 were observed in the liver than in plasma, with the pharmacokinetic profile mirroring that of the parent compound (Table 1; Table 2 in ESM-1).

In both rats and NHPs, hepatic metabolism was the primary route of elimination, and renal elimination was a minor route of clearance. The mean percentages of intact VIR-2218 detected in the urine were 11 and 10% of the total single subcutaneous dose in rats and NHPs, respectively, with the majority eliminated in the first 24 h. Only trace amounts of VIR-2218 were observed in urine samples collected over 24–168 h postdose. Overall, the favorable pharmacokinetic properties observed in the preclinical studies with the majority of the dose distributed to the liver support subcutaneous administration of VIR-2218 in human subjects.

3.2 VIR-2218 Phase I Clinical Study Population

A total of 49 healthy volunteers were enrolled and dosed in the study. One replacement subject was enrolled in the treatment group receiving 400 mg because the original subject withdrew consent. The baseline demographics across treatment arms were generally similar (Table 2). Among subjects receiving VIR-2218, 70% were women

Table 1 Mean liver pharmacokinetic parameters of VIR-2218 and AS(N-1)3' VIR-2218 after a single subcutaneous dose (10 mg/kg) in rats and nonhuman primates

Parameter	Rat		NHP	
	VIR-2218	AS (N-1)3' VIR-2218	VIR-2218	AS (N-1)3' VIR-2218
t_{\max} , h	7.0	24.0	24.0	72.0
C_{\max} , $\mu\text{g/g}$	97.0	45.9	135.0	51.5
AUC_{last} , $\text{h}^* \mu\text{g/g}$	6610	9910	37,200	28,600
$t_{1/2}$, h	93.1	147.0	160.0	806.5

AUC_{last} , area under curve from time of dosing to last measurable time point; C_{\max} , maximum concentration; NHP, nonhuman primates; $t_{1/2}$, half-life; t_{\max} , time to C_{\max}

Table 2 Demographics of healthy volunteers receiving single ascending doses of VIR-2218

Characteristic	VIR-2218							Placebo $n = 12$
	50 mg $n = 6$	100 mg $n = 6$	200 mg $n = 6$	400 mg $n = 7^a$	600 mg $n = 6$	900 mg $n = 6$	Overall $n = 37$	
Age, y	25 \pm 3	23 \pm 4	27 \pm 4	24 \pm 4	29 \pm 6	33 \pm 10	27 \pm 6	27 \pm 7
Male sex	0	2 (33)	3 (50)	0	3 (50)	3 (50)	11 (30)	7 (58)
Weight, kg	62 \pm 12	63 \pm 7	75 \pm 5	65 \pm 10	72 \pm 8	72 \pm 12	68 \pm 10	76 \pm 10
BMI, kg/m^2	23 \pm 5	23 \pm 3	24 \pm 2	25 \pm 4	26 \pm 1	26 \pm 4	25 \pm 3	24 \pm 2
Race								
Asian	2 (33)	3 (50)	0	0	2 (33)	1 (17)	8 (22)	1 (8)
White	2 (33)	2 (33)	5 (83)	5 (71)	3 (50)	3 (50)	20 (54)	8 (67)
Native Hawaiian or other Pacific Islander	1 (17)	1 (17)	0	1 (14)	0	0	3 (8)	2 (17)
Other	1 (17)	0	1 (17)	1 (14)	1 (17)	2 (33)	6 (16)	1 (8)

Data are presented as mean \pm standard deviation or n (%) unless otherwise indicated

BMI body mass index

^aIncludes replacement subject

with a mean age of 27 years and a mean BMI of 25 kg/m², whereas 42% of the subjects receiving placebo were women with a mean age of 27 years and a mean BMI of 24 kg/m².

3.3 Pharmacokinetics of VIR-2218 and AS(N-1)3'VIR-2218 in Healthy Volunteers

3.3.1 Plasma Pharmacokinetics

The VIR-2218 plasma concentration profiles indicate rapid absorption and elimination from the systemic circulation, with plasma concentrations declining below LLOQ beyond 48 h in any subject (Fig. 2), which is consistent with rapid GalNAc-mediated uptake into the liver [15, 16, 21]. The plasma pharmacokinetic profile of AS(N-1)3'VIR-2218 mirrored that of VIR-2218. AS(N-1)3'VIR-2218 was quantifiable only at doses \geq 100 mg and was not quantifiable in plasma beyond 12 h for most subjects (27 of 35) and beyond 24 h in any subject (Fig. 2b). The median t_{\max} of VIR-2218 occurred between 4 and 7 h, and the median t_{\max} of AS(N-1)3'VIR-2218 occurred between 6 and 10 h (Table 3). The median $t_{1/2}$ of VIR-2218 was approximately 2–5 h. Systemic exposures of VIR-2218 were characterized by low-to-moderate interindividual variability (%CV was $<$ 32% for AUC; $<$ 43% for C_{\max}).

Because both VIR-2218 and AS(N-1)3'VIR-2218 were detectable up to 12 h in most subjects, the mean \pm standard deviation of the AUC₀₋₁₂ was used for comparison across VIR-2218 and metabolite as well as across dosing cohorts. The metabolite to parent ratio (MR) for C_{\max} and AUC₀₋₁₂ was \leq 12% in the evaluated dose range of 100–900 mg. Because of the low concentrations and short half-life of AS(N-1)3'VIR-2218 in plasma and the pharmacokinetic sampling schedule limitations, λ_z was not calculable; therefore, values of the associated parameters ($t_{1/2}$, AUC _{∞} , CL/F, and apparent V_z/F) were not reported.

3.3.2 Dose Proportionality

VIR-2218 plasma exposures (AUC₀₋₁₂, AUC _{∞} , and C_{\max}) increased with dose. The estimated slope (β) or proportionality coefficients were 1.19 (90% CI 1.10–1.28), 1.24 (90% CI 1.16–1.31), and 1.16 (90% CI 1.06–1.26) for AUC₀₋₁₂, AUC _{∞} , and C_{\max} , respectively (Fig. 3a–c), indicating a slightly greater-than-dose-proportional increase in plasma exposures across the studied dose range of 50–900 mg. A similar trend was observed with the active metabolite AS(N-1)3'VIR-2218 (data not shown).

3.3.3 Urine Pharmacokinetics

Concentrations of VIR-2218 and AS(N-1)3'VIR-2218 were detected in urine through the last measured time point at 1 week post dose in all cohorts. The pharmacokinetic profile of VIR-2218 and AS(N-1)3'VIR-2218 in urine mirrored that in plasma up to 48 h.

The urine pharmacokinetic parameters after single subcutaneous doses of VIR-2218 are shown in Table 4. Over the initial 24-h period, approximately 17–48 and 2–7% of the administered dose (50–900 mg) was excreted in urine as unchanged VIR-2218 and AS(N-1)3'VIR-2218, respectively, with the majority of the drug excreted within the first 12 h. The fraction of VIR-2218 excreted in urine over 24 h post dose increased with dose level (Fig. 4). At doses up to 600 mg, 19–36% of parent and metabolite was excreted in urine within 24 h postdose, whereas that proportion increased to 55% at a dose of 900 mg. The mean CL_R of VIR-2218 ranged from 5.13 to 7.47 L/h (mean 6.5 L/h; Table 4), and the mean CL/F ranged from 15 to 34 L/h (Table 3). The fraction of renal clearance to total clearance (CL_R/CL/F) ranged from 17.3 to 48.8% in the dose range of 50–900 mg after single subcutaneous injection.

Fig. 2 Plasma concentration vs. time profiles for VIR-2218 and AS(N-1)3'VIR-2218 after a single subcutaneous dose in healthy volunteers. For plotting purposes, BLQ values in subjects were included as 0. Subjects with all BLQ values were excluded. BLQ, below limit of quantitation; SD, standard deviation

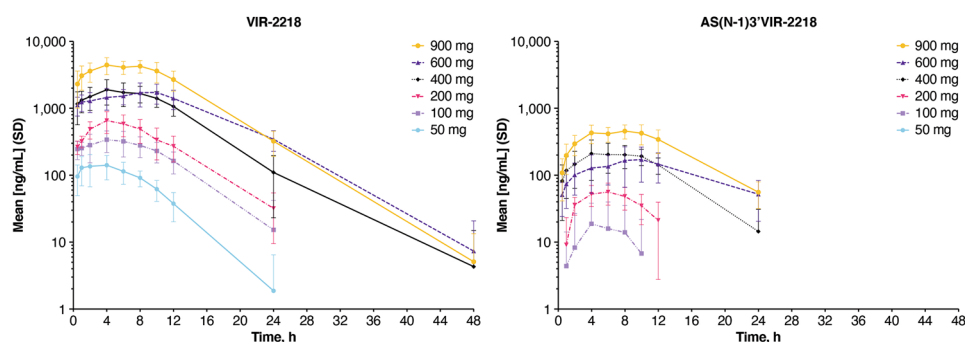


Table 3 Plasma pharmacokinetic parameters for VIR-2218 and AS(N-1)3'VIR-2218 after single subcutaneous dose in healthy volunteers

Parameter	50 mg <i>n</i> = 6	100 mg <i>n</i> = 5 ^a	200 mg <i>n</i> = 6	400 mg <i>n</i> = 6 ^{a,b}	600 mg <i>n</i> = 6	900 mg <i>n</i> = 6
VIR-2218						
AUC ₀₋₁₂ , h ng/mL	1200 (25.1)	3230 (32.7)	5470 (28.0)	18,100 (24.2)	17,500 (30.8)	44,100 (17.9)
AUC _{last} , h ng/mL	1270 (21.2)	3740 (31.8)	6630 (17.6)	23,500 (11.5)	27,900 (27.0)	58,800 (15.4)
AUC _∞ , h ng/mL	1480 (8.0)	4730 (19.2)	6600 (13.6) ^c	24,000 (10.2)	29,600 (28.5)	60,000 (14.9)
C _{max} , ng/mL	155 (42.1)	355 (32.9)	711 (29.2)	2110 (34.3)	1830 (33.5)	5010 (12.6)
<i>t</i> _{max} , h	4.25 (1.17; 4.25)	4.32 (4.25; 6.17)	5.21 (4.25; 6.18)	7.21 (4.25; 8.25)	7.21 (6.17; 10.2)	4.25 (4.25; 8.25)
<i>t</i> _{last} , h	12.3 (12.3; 12.3)	12.3 (12.3; 24.3)	24.3 (24.3; 24.3)	24.3 (24.3; 24.3)	24.3 (24.3; 48)	24.3 (24.3; 48)
<i>t</i> _{1/2} , h	2.45 (2.35; 3.26)	3.64 (3.49; 4.95)	4.38 (4.22; 6.11) ^c	3.54 (2.49; 5.51)	5.28 (5.12; 5.62)	4.55 (3.25; 4.69)
CL/F, L/h	34.0 (7.5)	21.8 (19.6)	30.8 (14.6)	16.8 (10.5)	21.9 (31.6)	15.3 (13.6)
V _Z /F, L	155 (44.9)	132 (30.9)	223 (34.0)	104 (60.4)	176 (34.5)	92.9 (26.5)
AS(N-1)3'VIR-2218						
AUC ₀₋₁₂ , h ng/mL	BLQ	NC	513 (27.2)	2110 (38.1)	1580 (52.4)	4440 (23.3)
AUC _{last} , h ng/mL	BLQ	208 (91.5) ^d	481 (31.0)	2530 (24.2)	2680 (54.6)	6430 (23.3)
C _{max} , ng/mL	BLQ	40.5 (48.2) ^d	62.4 (28.2)	259.0 (44.0)	177.0 (55.9)	514.0 (20.6)
<i>t</i> _{max} , h	NC	6.17 (4.25; 6.17) ^d	6.17 (4.25; 6.18)	9.21 (4.25; 10.2)	10.2 (8.25; 10.2)	8.25 (4.25; 10.2)
<i>t</i> _{last} , h	NC	8.3 (4.25; 10.2) ^d	12.3 (10.2; 12.3)	18.3 (12.3; 24.3)	24.3 (24.3; 24.3)	24.3 (24.3; 24.3)
MR						
MR _{Cmax}	NC	0.0892 ^d	0.0886	0.121	0.0918	0.102
MR _{AUC0-12}	NC	NC	0.0891 ^c	0.114	0.0851	0.100

Time parameters are expressed as median (Q1; Q3); all other data are arithmetic mean (%CV). When *n* < 3, the CV is not presented. Because of short VIR-2218 *t*_{1/2} and pharmacokinetic sampling schedule limitations, the terminal phase was not adequately characterized for the metabolite; therefore, apparent clearance and *t*_{1/2} are not reported

AUC, area under the plasma concentration–time curve; AUC₀₋₁₂, AUC from time 0 to 12 h; AUC_∞, AUC extrapolated to infinity; AUC_{last}, AUC from time of dosing to last measurable time point; BLQ, below limit of quantitation; CL/F, apparent plasma clearance; C_{max}, maximum concentration; CV, coefficient of variation; MR, metabolite to parent ratio; NC, not calculable; Q, quartile; *t*_{1/2}, half-life; *t*_{last}, last measurable time; *t*_{max}, time to C_{max}; V_Z/F, apparent volume of distribution

^aExcludes one subject who received a partial dose

^bIncludes pharmacokinetics from one replacement subject

^cMeasurable in five of six subjects

^dMeasurable in three of six subjects

4 Discussion

VIR-2218 is an ESC+ GalNAc–siRNA conjugate in development for the treatment of chronic HBV infection. VIR-2218 is designed to target and downregulate all HBV transcripts to reduce viral antigens driving chronic HBV infection, offering a potential curative treatment option. The purpose of this report was to characterize the single-dose pharmacokinetics of VIR-2218 in rats, NHPs, and healthy volunteers. VIR-2218 was absorbed after subcutaneous administration and detectable as early as 30 minutes post dose, with maximum concentrations reached by 4–7 h post dose. VIR-2218 was converted to its metabolite AS(N-1)3'VIR-2218, and metabolite concentrations were ~tenfold lower than the parent. The short plasma half-life of VIR-2218 and AS(N-1)3'VIR-2218 is attributable to the rapid and specific ASGPR-mediated uptake into the liver [13, 14]. VIR-2218 is expected to be stable in plasma as

ESC+ modifications reduce its susceptibility to nuclease-mediated cleavage and enhance its stability in the systemic circulation. Similarly, in vitro studies of GalNAc–siRNA conjugates showed robust uptake into hepatocytes with minimal degradation after 24 h of incubation [13, 14]. The effect of VIR-2218 on HBsAg reduction is expected to be durable because of its enhanced metabolic stability, selective uptake into the liver, and potential long residence time in hepatocytes.

In preclinical studies in rats and NHPs, VIR-2218 was stable in plasma and was similarly metabolized to AS(N-1)3'VIR-2218, which was the most prominent circulating metabolite and < 10% of the full-length antisense strand exposure. After administration of a single subcutaneous dose of 10 mg/kg, VIR-2218 rapidly distributed to the liver, reaching peak liver concentrations within 7 and 24 h in rats and NHPs, respectively. VIR-2218 and AS(N-1)3'VIR-2218 exhibited much higher exposures and longer

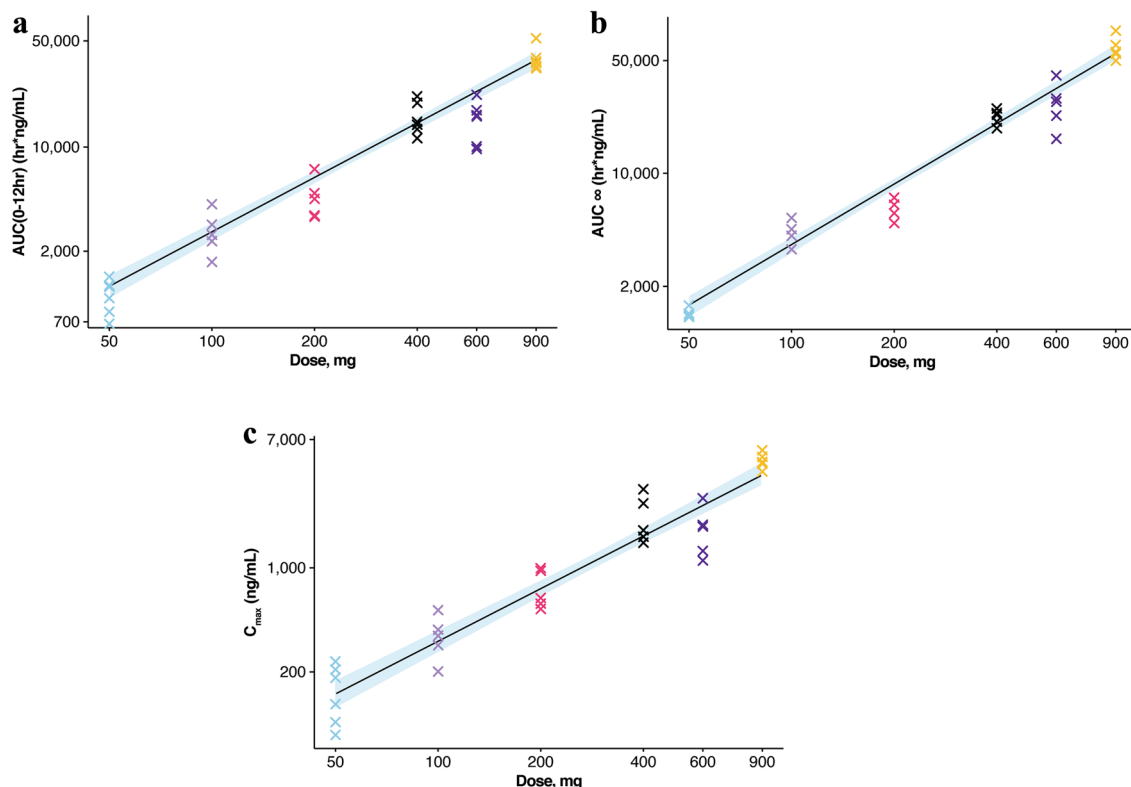


Fig. 3 Plasma VIR-2218 dose proportionality from 50 to 900 mg after single subcutaneous VIR-2218 administration. VIR-2218 dose vs. **a** AUC_{0-12} , **b** AUC_{∞} , and **c** C_{max} on a logarithmic scale. The estimated slope (β) or proportionality coefficients were 1.19 (90% CI 1.10–1.28), 1.24 (90% CI 1.16–1.31), and 1.16 (90% CI 1.06–1.26) for AUC_{0-12} , AUC_{∞} , and C_{max} , respectively. Crosses denote indi-

vidual pharmacokinetic parameters, and the estimated slope is the proportionality coefficient. The shaded area represents the 90% CIs around the regression line. AUC_{0-12h} , area under the plasma concentration–time curve from time 0 to 12 h; AUC_{∞} , AUC extrapolated to infinity; CI, confidence interval; C_{max} , maximum concentration; PK, pharmacokinetics

Table 4 Urine pharmacokinetic parameters for VIR-2218 and AS(N-1)3'VIR-2218 over 24 h postdose

Pharmacokinetic parameter	50 mg <i>n</i> = 6	100 mg <i>n</i> = 5 ^a	200 mg <i>n</i> = 6	400 mg <i>n</i> = 6 ^{a,b}	600 mg <i>n</i> = 6	900 mg <i>n</i> = 6
VIR-2218						
Plasma AUC_{0-24} , h·ng/mL	1460 (9.5) ^c	4530 (19.7) ^c	6290 (14.6)	23,100 (14.0)	26,800 (29.4)	57,800 (15.8)
CL_R/F , L/h	5.87 (12.4)	5.22 (24.3)	7.00 (9.4)	5.13 (16.6)	7.22 (20.5)	7.47 (17.9)
Urine f_{e0-24} , %	16.9 (18.8)	21.7 (28.6)	23.2 (18.7)	29.5 (19.4)	32.3 (36.4)	47.6 (18.0)
AS(N-1)3'VIR-2218						
Urine f_{e0-24} , %	1.94 (24.8)	4.16 (54.9)	3.31 (19.8)	4.99 (14.8)	4.12 (56.2)	6.96 (21.2)

All pharmacokinetic parameters are expressed as arithmetic mean (% coefficient of variation)

AUC_{0-24} , area under curve from time 0–24 h; CL_R/F , apparent renal clearance from 0–24 h; f_{e0-24} , fraction excreted from time 0 to 24 h

^aExcludes one subject who received a partial dose

^bIncludes pharmacokinetics from the replacement subject

^c AUC_{0-24} is extrapolated

residence times in the liver than in plasma in both rats and NHPs, which is consistent with efficient ASGPR-mediated uptake into hepatocytes and similar to other GalNAc–siRNA conjugates [15, 16, 21]. Prolonged residence

of VIR-2218 within hepatocytes was further evidenced by an extended mean liver $t_{1/2}$ of 93.1 h in rats and 160.0 h in NHPs. Renal excretion of VIR-2218 was 11% of the administered dose in rats and approximately 10% in NHPs.

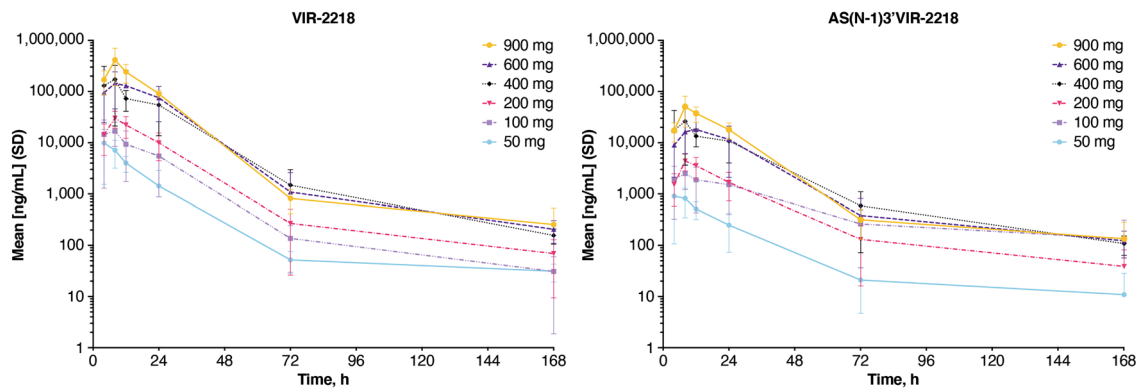


Fig. 4 Urine concentration vs. time profiles for VIR-2218 and AS(N-1)3'VIR-2218. For plotting purposes, the BLQ value in subjects was included as 0. Subjects with all BLQ values were excluded. BLQ, below limit of quantitation; SD, standard deviation

These data suggest that, in both rats and NHPs, uptake by the liver and subsequent metabolism is the primary route of systemic clearance. Thus, the subsequent high liver concentration and long residence time of VIR-2218 in liver are expected to confer extended pharmacodynamic effects.

In healthy volunteers in the VIR-2218 phase I clinical study, after administration of VIR-2218 doses up to 600 mg, renal excretion was a minor route of VIR-2218 elimination, with 19–36% of parent and metabolite excreted in urine within 24 h postdose, whereas the majority of the drug localized to the liver with ASGPR-mediated uptake. A different excretion profile was observed at the dose of 900 mg, with 55% of parent and metabolite excreted in urine within 24 h. The fraction of unchanged VIR-2218 excreted in urine increased with dose, consistent with slightly greater than dose-proportional increases in plasma exposures at the 900-mg dose and suggestive of transient saturation of ASGPR at high doses [15]. Efficient liver targeting and uptake was shown with a preclinical study in rats that found that > 77% of subcutaneous GalNAc–siRNA conjugate was localized in the liver [13]. Furthermore, results from *in vitro* studies using freshly isolated primary hepatocytes showed that GalNAc–siRNA conjugates were robustly taken up into hepatocytes [14]. The clinical pharmacokinetics of VIR-2218 are consistent with those of GalNAc–conjugated siRNAs, suggesting high liver exposure and prolonged residence within the liver, which secondarily is anticipated to yield a sustained systemic pharmacodynamic effect.

Consistent with rapid GalNAc-mediated liver uptake, VIR-2218 was short lived in plasma in healthy volunteers, with a median $t_{1/2}$ of 2–5 h post administration and plasma concentrations below the level of quantitation beyond 48 hours in all subjects. The short half-life of VIR-2218 and the expected limitations of the pharmacokinetic sampling schedule and pharmacokinetic assay sensitivity could lead to bias in the estimation of the terminal phase, $t_{1/2}$, and CL/F of VIR-2218 and metabolite.

The pharmacokinetic/pharmacodynamic (PK/PD) properties of other investigational GalNAc–conjugated RNA therapeutics support the potential for a prolonged pharmacodynamic effect with VIR-2218. For instance, a single subcutaneous dose of vutrisiran, under development for transthyretin-mediated amyloidosis, resulted in robust reduction of transthyretin in healthy volunteers and was maintained for months [16]. Similarly, cemdisiran, an RNA therapeutic for the treatment of complement-mediated diseases, showed robust target suppression (complement 5 protein) persisting up to 13 months after a single subcutaneous dose [21]. Thus, the potential prolonged presence of VIR-2218 in hepatocytes is expected to bring about long-lasting inhibition of secretion of HBV virions and production of subviral HBV particles, leading to enduring pharmacodynamic effects on the reduction of HBsAg. This has been demonstrated for GalNAc–siRNA conjugates in preclinical studies, showing a strong correlation between total siRNA levels in liver and silencing activity [13].

In preclinical species, VIR-2218 plasma concentrations did not directly correlate with efficacy (HBsAg decline) because HBsAg continued to decline even after VIR-2218 was undetectable in plasma (Vir Biotechnology, Inc., unpublished data). This was further illustrated by the differences in plasma versus liver $t_{1/2}$ of VIR-2218: the drug was still efficacious long after its disappearance from plasma. As a result, the decline of HBsAg following multiple doses of VIR-2218 is being assessed in current clinical studies to determine the relationship between HBsAg decline, dose, and duration of VIR-2218 in subjects with HBV and will be used to develop a clinical PK/PD model to guide clinical dosing regimens of VIR-2218 in future studies.

Favorable plasma and urine pharmacokinetic profiles and the potential prolonged liver localization of VIR-2218 in humans are consistent with those of other

GalNAc–siRNA conjugates and support continued clinical development of VIR-2218. Furthermore, no severe or serious adverse events or discontinuations due to adverse events were observed within the dose range evaluated for VIR-2218 in healthy volunteers. The safety data for VIR-2218 will be described in a separate publication (Vir Biotechnology, Inc., unpublished data). Overall, these results support the continued therapeutic development of VIR-2218 as a potential backbone for a finite treatment regimen aimed at a functional cure for chronic HBV infection.

5 Conclusions

VIR-2218 was rapidly absorbed and eliminated from the systemic circulation after subcutaneous dosing, with VIR-2218 and its primary metabolite AS(N-1)3' VIR-2218 undetectable in plasma after 48 and 24 h, respectively, attributable to rapid GalNAc-mediated uptake into the liver. Based on the prolonged presence of VIR-2218 in the urine of healthy volunteers and the tissue pharmacokinetics in preclinical species, VIR-2218 was targeted to liver via the ASGPR receptor and exhibited extended exposure in the target tissue, consistent with PK/PD properties of other GalNAc-conjugated siRNA molecules. At single doses up to 600 mg, renal clearance was a minor route of VIR-2218 elimination. The favorable pharmacokinetic results and safety profile support continued evaluation and therapeutic development of VIR-2218 for subcutaneous administration in chronic HBV infection.

Supplementary Information The online version contains supplementary material available at <https://doi.org/10.1007/s40268-021-00369-w>.

Acknowledgements Professional medical writing assistance was provided by Magdalena Kalinowska, PhD, and Vanisha Lakhina, PhD, of VMLY&R. Funding for this manuscript was provided by Vir Biotechnology, Inc. Special thanks to the VIR-2218-1001 study volunteers, site coordinators, and study investigators.

Declarations

Funding This work was supported by Vir Biotechnology, Inc. and Alnylam Pharmaceuticals, Inc., who contributed to the study design, research, and interpretation of data and the writing, review, and approval of the manuscript for publication.

Conflicts of interest Sneha V. Gupta, Marie C. Fanget, Daniel Cloutier, Ling Shen, and Erik Mogalian are or were employees of Vir Biotechnology, Inc. and may hold Vir stocks or options. Christopher MacLauchlin, Valerie A. Clausen, Jing Li, and Gabriel J. Robbie are or were employees of Alnylam Pharmaceuticals, Inc. and may hold Alnylam stocks or options.

Ethics approval This study was conducted according to the International Conference on Harmonization for Good Clinical Practice, the Declaration of Helsinki, and all applicable federal and local regulations. The study was approved by central and local institutional review boards.

Consent to participate Written informed consent was obtained from each subject before any study-related procedures were performed.

Consent for publication The authors, jointly and severally, give the publisher the permission to publish the work. Subjects signed informed consent regarding publishing their data.

Availability of data and material The authors declare that the data supporting the findings of this study are available within the article and its supplementary information files.

Code availability Not applicable.

Author contributions Data collection and analysis were performed by Sneha V. Gupta, Marie C. Fanget, Christopher MacLauchlin, Valerie A. Clausen, Jing Li, and Erik Mogalian. Sneha V. Gupta, Marie C. Fanget, Christopher MacLauchlin, Valerie A. Clausen, Jing Li, Daniel Cloutier, Ling Shen, Gabriel J. Robbie, and Erik Mogalian contributed to the study conceptualization and design, interpretation of results, and writing and reviewing of the manuscript.

Open Access This article is licensed under a Creative Commons Attribution-NonCommercial 4.0 International License, which permits any non-commercial use, sharing, adaptation, distribution and reproduction in any medium or format, as long as you give appropriate credit to the original author(s) and the source, provide a link to the Creative Commons licence, and indicate if changes were made. The images or other third party material in this article are included in the article's Creative Commons licence, unless indicated otherwise in a credit line to the material. If material is not included in the article's Creative Commons licence and your intended use is not permitted by statutory regulation or exceeds the permitted use, you will need to obtain permission directly from the copyright holder. To view a copy of this licence, visit <http://creativecommons.org/licenses/by-nc/4.0/>.

References

1. Trepo C. A brief history of hepatitis milestones. *Liver Int.* 2014;34(Suppl 1):29–37. <https://doi.org/10.1111/liv.12409>.
2. Schweitzer A, Horn J, Mikolajczyk RT, Krause G, Ott JJ. Estimations of worldwide prevalence of chronic hepatitis B virus infection: a systematic review of data published between 1965 and 2013. *Lancet.* 2015;386(10003):1546–55. [https://doi.org/10.1016/S0140-6736\(15\)61412-X](https://doi.org/10.1016/S0140-6736(15)61412-X).
3. Stanaway JD, Flaxman AD, Naghavi M, Fitzmaurice C, Vos T, Abubakar I, et al. The global burden of viral hepatitis from 1990 to 2013: findings from the Global Burden of Disease Study 2013. *Lancet.* 2016;388(10049):1081–8. [https://doi.org/10.1016/S0140-6736\(16\)30579-7](https://doi.org/10.1016/S0140-6736(16)30579-7).
4. Nelson NP, Easterbrook PJ, McMahon BJ. Epidemiology of hepatitis B virus Infection and impact of vaccination on disease. *Clin Liver Dis.* 2016;20(4):607–28. <https://doi.org/10.1016/j.cld.2016.06.006>.
5. Kramvis A. Genotypes and genetic variability of hepatitis B virus. *Intervirology.* 2014;57(3–4):141–50. <https://doi.org/10.1159/000360947>.

6. Protzer U, Maini MK, Knolle PA. Living in the liver: hepatic infections. *Nat Rev Immunol*. 2012;12(3):201–13. <https://doi.org/10.1038/nri3169>.
7. Liang TJ, Block TM, McMahon BJ, Ghany MG, Urban S, Guo JT, et al. Present and future therapies of hepatitis B: from discovery to cure. *Hepatology*. 2015;62(6):1893–908. <https://doi.org/10.1002/hep.28025>.
8. Scaglione SJ, Lok AS. Effectiveness of hepatitis B treatment in clinical practice. *Gastroenterology*. 2012;142(6):1360–8. <https://doi.org/10.1053/j.gastro.2012.01.044>.
9. Konerman MA, Lok AS. Interferon treatment for hepatitis B. *Clin Liver Dis*. 2016;20(4):645–65. <https://doi.org/10.1016/j.cld.2016.06.002>.
10. Agrawal N, Dasaradhi PV, Mohammed A, Malhotra P, Bhatnagar RK, Mukherjee SK. RNA interference: biology, mechanism, and applications. *Microbiol Mol Biol Rev*. 2003;67(4):657–85. <https://doi.org/10.1128/mmb.67.4.657-685.2003>.
11. Fire A, Xu S, Montgomery MK, Kostas SA, Driver SE, Mello CC. Potent and specific genetic interference by double-stranded RNA in *Caenorhabditis elegans*. *Nature*. 1998;391(6669):806–11. <https://doi.org/10.1038/35888>.
12. Soutschek J, Akinc A, Bramlage B, Charisse K, Constien R, Donoghue M, et al. Therapeutic silencing of an endogenous gene by systemic administration of modified siRNAs. *Nature*. 2004;432(7014):173–8. <https://doi.org/10.1038/nature03121>.
13. Nair JK, Attarwala H, Sehgal A, Wang Q, Aluri K, Zhang X, et al. Impact of enhanced metabolic stability on pharmacokinetics and pharmacodynamics of GalNAc-siRNA conjugates. *Nucleic Acids Res*. 2017;45(19):10969–77. <https://doi.org/10.1093/nar/gkx818>.
14. Nair JK, Willoughby JL, Chan A, Charisse K, Alam MR, Wang Q, et al. Multivalent N-acetylgalactosamine-conjugated siRNA localizes in hepatocytes and elicits robust RNAi-mediated gene silencing. *J Am Chem Soc*. 2014;136(49):16958–61. <https://doi.org/10.1021/ja505986a>.
15. Agarwal S, Simon AR, Goel V, Habtemariam BA, Clausen VA, Kim JB, et al. Pharmacokinetics and pharmacodynamics of the small interfering ribonucleic acid, givosiran, in patients with acute hepatic porphyria. *Clin Pharmacol Ther*. 2020;108(1):63–72. <https://doi.org/10.1002/cpt.1802>.
16. Habtemariam BA, Karsten V, Attarwala H, Goel V, Melch M, Clausen VA, et al. Single-dose pharmacokinetics and pharmacodynamics of transthyretin targeting N-acetylgalactosamine-small interfering ribonucleic acid conjugate, vutrisiran, in healthy subjects. *Clin Pharmacol Ther*. 2021;109(2):372–82. <https://doi.org/10.1002/cpt.1974>.
17. Schwartz AL, Rup D, Lodish HF. Difficulties in the quantification of asialoglycoprotein receptors on the rat hepatocyte. *J Biol Chem*. 1980;255(19):9033–6.
18. Willoughby JLS, Chan A, Sehgal A, Butler JS, Nair JK, Racie T, et al. Evaluation of galNAc-siRNA conjugate activity in pre-clinical animal models with reduced asialoglycoprotein receptor expression. *Mol Ther*. 2018;26(1):105–14. <https://doi.org/10.1016/j.ymthe.2017.08.019>.
19. Smith BP, Vandenhende FR, DeSante KA, Farid NA, Welch PA, Callaghan JT, et al. Confidence interval criteria for assessment of dose proportionality. *Pharm Res*. 2000;17(10):1278–83. <https://doi.org/10.1023/a:1026451721686>.
20. Manoharan M. RNA interference and chemically modified small interfering RNAs. *Curr Opin Chem Biol*. 2004;8(6):570–9. <https://doi.org/10.1016/j.cbpa.2004.10.007>.
21. Badri P, Jiang X, Borodovsky A, Najafian N, Kim J, Clausen VA, et al. Pharmacokinetic and pharmacodynamic properties of cemdisiran, an RNAi therapeutic targeting complement component 5, in healthy subjects and Patients with Paroxysmal Nocturnal Hemoglobinuria. *Clin Pharmacokinet*. 2020. <https://doi.org/10.1007/s40262-020-00940-9>.

Authors and Affiliations

Sneha V. Gupta¹ · Marie C. Fanget² · Christopher MacLauchlin⁵ · Valerie A. Clausen⁶ · Jing Li⁶ · Daniel Cloutier³ · Ling Shen⁴ · Gabriel J. Robbie⁷ · Erik Mogalian¹

¹ Clinical Pharmacology, Vir Biotechnology, Inc., San Francisco, CA, USA

² Bioanalytical Sciences, Vir Biotechnology, Inc., San Francisco, CA, USA

³ Clinical Research, Vir Biotechnology, Inc., San Francisco, CA, USA

⁴ Biometrics, Vir Biotechnology, Inc., San Francisco, CA, USA

⁵ Drug Metabolism and Pharmacokinetics, Alnylam Pharmaceuticals, Inc., Cambridge, MA, USA

⁶ Bioanalytical Sciences, Alnylam Pharmaceuticals, Inc., Cambridge, MA, USA

⁷ Clinical Pharmacology and Pharmacometrics, Alnylam Pharmaceuticals, Inc., Cambridge, MA, USA